CHAPTER 11.6
MICROWAVE AMPLIFIERS AND OSCILLATORS

John W. Lunden, Jennifer E. Doyle

MICROWAVE SOLID-STATE DEVICES

Since the 1950s, solid-state devices have replaced tubes in most amplifier and oscillator applications. Solid-state devices are preferred because of better long-term reliability, lower cost, and improved noise characteristics. In the 1960s and 1970s, avalanche and Gunn diodes were used extensively in the generation of microwave power.

More recently, junction and field-effect transistors have been increasingly used in microwave amplifiers and oscillators. Gallium arsenide (GaAs) FETs have replaced other solid-state devices in many microwave applications; however, impact ionization avalanche transit-time (IMPATT) and Gunn diodes are still commonly used at frequencies above 20 GHz.

IMPATT DIODE CIRCUITS

The generation of microwave power in a reverse-biased *pn* junction was originally suggested by Read (1958). He proposed that the finite delay between applied rf voltage and the current generated by avalanche breakdown, with the subsequent drift of the generated carriers through the depletion layer of the junction, would lead to negative resistance at microwave frequencies. The diode is biased in the avalanche-breakdown region. As the rf voltage rises above the dc breakdown voltage during the positive half cycle, excess charge builds up in the avalanche region, reaching a peak when the rf voltage is zero. Hence this charge waveform lags the rf voltage by 90°. Subsequently, the direction of the field in the diode causes the multiplied carriers to drift across the depletion region. This, in turn, induces a positive current in the external circuit while the diode rf voltage is going through its negative half cycle. This is equivalent to negative resistance, which is maximum when the transit angle is approximately 0.74π.

A simplified equivalent circuit of the IMPATT diode circuit is shown in Fig. 11.6.1. The resistance R_D includes both the parasitic positive resistance because of contacts, bulk material, and so forth, and the dynamic negative resistance. The net magnitude is typically in the range –0.5 to –4.0 Ω and varies with current. The capacitance C_D is the voltage-sensitive depletion-layer capacitance and can be approximated sufficiently accurately with the value at breakdown. The diode resistance variation results in a stable operating point for any positive load resistance equal to or less than the diode's peak negative value.

Oscillations will build up and be maintained at the frequency for which the net inductive reactance of the package parasitics and the external load equals the capacitive reactance of C_D. The values for L_P and C_P vary

with package or mounting style. Typical values range from 0.3 to 0.6 nH and 0.2 to 0.4 pF, respectively. It is important to minimize these parasitics since they limit the operating frequency and band-width.

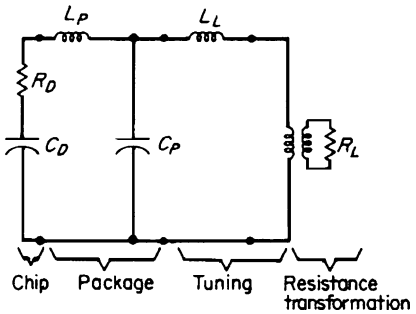

FIGURE 11.6.1 Approximate rf equivalent circuit of IMPATT oscillator.

IMPATT diodes can be used in several mounting configurations, including coaxial, waveguide, strip-line, or microstrip. It is important to ensure that a good heat flow path is provided (owing to the typically low efficiency) and that low-electrical-resistance contacts be made to both anode and cathode.

In avalanche breakdown, the diode tends to look like a voltage source. Hence a current source is desirable for dc bias. Several circuits are possible. The *RC* bias circuit (Fig. 11.6.2*a*) is the simplest but is inefficient, and the transistor current regulator (Fig. 11.6.2*b*) may be more desirable. In either case, the loading of the diode with shunt capacitance or a resonance path to ground (at some frequency) must be avoided to prevent instabilities (noise and/or spurious frequencies).

Two broadly tunable diode loading circuits are the multiple-slug cavity and the variable-package-inductance types. Coaxial implementations of these two techniques are shown in the cross sections of Fig. 11.6.3. In Fig. 11.6.3*a* slugs $\lambda/8$ and/or $\lambda/4$ long at the desired center frequency of operation with characteristic impedance of between 10 and 20 Ω are adjusted in position along the centerlines to provide a load reactance equal to the negative of the diode reactance and a load resistance equal to or less than the magnitude of the diode net negative resistance. Circuit *b* tunes the diode by recessing it into the holder, effectively decreasing the net series inductance, which is resonant with the diode capacitance. Single- or multisection transformers can also be included for resistive matching to the load R_L. Similar waveguide-circuit implementations can be used with typically narrower bandwidths, better frequency stability, and lower FM noise.

The IMPATT diode can function as an amplifier if the load resistance presented to it is larger in magnitude than the negative resistance of the diode. Typically, a circulator is used in conjunction with the tuned diode circuit to separate input and output signals. At the center frequency, the power gain of the amplifier is given by

$$G_0 = \left(\frac{R_D - R_L}{R_D + R_L} \right)^2$$

where R_D and R_L are as shown in Fig. 11.6.1.

In general, amplifier operation for a given diode requires a smaller shunt tuning capacitor or a large transformer characteristic impedance. An estimate of the diode rf current and voltage can be obtained from

$$V_D \approx \frac{\sqrt{2P_o R_L}}{\omega C_j(V_b)} \left(1 + \frac{1}{\sqrt{G_0}} \right) \qquad I_D \approx \omega C_j(V_b) V_D$$

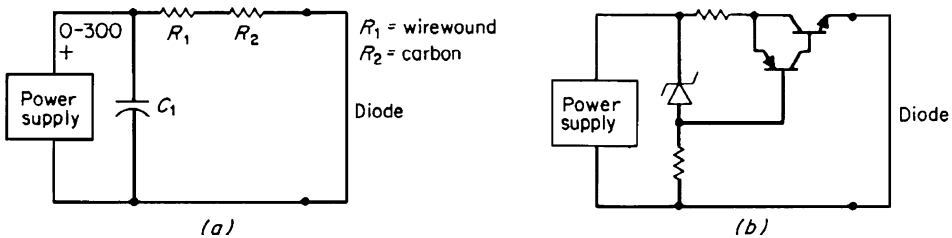

FIGURE 11.6.2 Bias circuits for IMPATT diodes: (*a*) *RC* type; (*b*) transistor-regulated type.

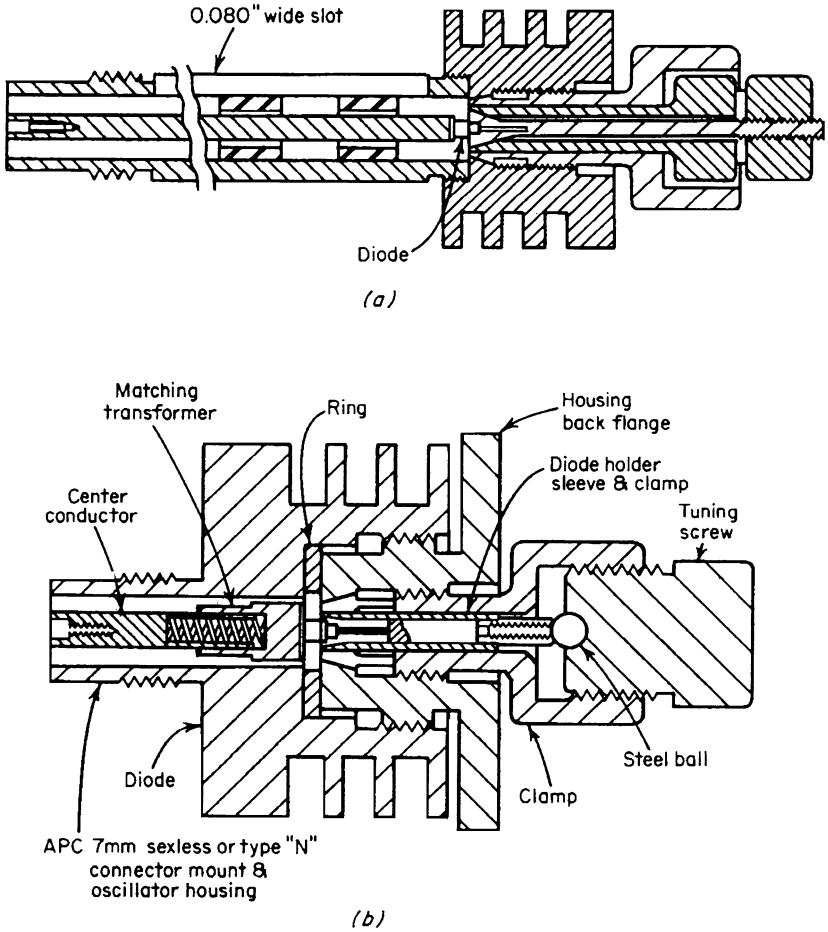

FIGURE 11.6.3 Mechanical tuning of IMPATT circuit: (*a*) multiple-slug type; (*b*) variable-inductance (diode-recess) type. (*Hewlett-Packard Company*.)

where V_b = diode breakdown voltage
C_j = junction capacitance
P_o = power output
G_0 = gain

Higher output powers have been achieved by multiple-diode series-parallel configurations and/or hybrid combining techniques.

In general, properly designed IMPATT oscillator circuits can have noise performance comparable with reflex klystron or Gunn oscillators. The noise performance of both Si and GaAs IMPATT diode amplifiers and oscillators has been extensively treated in the literature.

IMPATT diodes are usable at higher frequencies than any other solid-state device currently available. Silicon IMPATT diodes can be used at frequencies as high as 300 GHz. Some of the disadvantages of IMPATTS are a low gain-bandwidth product, difficult adjustments necessary for long-term performance reliability, bias circuit instabilities, and inherent nonlinearity. The cw power output achievable with a single

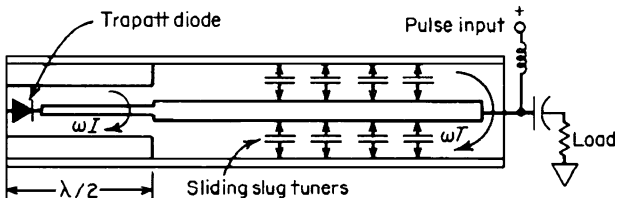

FIGURE 11.6.4 Typical TRAPATT diode circuit configuration.

IMPATT diode is 3 W at 11 GHz, 2 W at 15 GHz, or 1 W at 20 GHz. Diodes can be paralleled to obtain higher power, for example, 10 W at 41 GHz, with 30 dB gain and 250 MHz bandwidth, by combining 12 diodes in one cavity.

TRAPATT DIODE CIRCUITS

The trapped plasma avalanche triggered transit (TRAPATT) mode of operation is characterized by high efficiency, operation at frequencies well below the transit-time frequency, and a significant change in the dc operating point when the diode switches into the mode. The basic understanding of this high-efficiency mode of operation has proceeded from consideration of IMPATT diode behavior with large signals. Two saturation mechanisms in the IMPATT diode, space-charge suppression of the avalanche and carrier trapping, reduce the power generated at the transit-time frequency, but play an important role in establishing the "trapped-plasma" states for high-efficiency operation.

To manifest the high efficiency of the TRAPATT mode, four important circuit conditions must be met: large IMPATT-generated voltage swings must be obtained by trapping the IMPATT oscillation in a high-Q-cavity circuit; selective reflection and/or rejection of all subharmonics of the IMPATT frequency except the desired subharmonics must be realized (typically with a low-pass filter); sufficient capacitance must be provided near the diode to sustain the high-current state; and tuning or matching to the load must be provided at the TRAPATT frequency. Figure 11.6.4 illustrates a widely used circuit that achieves the foregoing conditions.

The TRAPATT diode is typically represented by a current pulse generator and the diode's depletion-layer capacitance, as shown in the simplified schematic of Fig. 11.6.5. This permits a simple interpretation of operation. Initially, a large voltage pulse reaches the diode, triggering the traveling avalanche zone in the diode. This initiates a high-current low-voltage state. The drop in voltage propagates down the line l, is inverted (owing to the –1 reflection coefficient of the low-pass filter), and travels back toward the diode. The process then repeats. Consequently, the frequency of operation is inversely proportional to the length of line l. The period of oscillation is slightly modified by the finite time required for the diode voltage to drop to zero. The inductance L is a result of the bond lead and is helpful in driving the diode voltage high enough to initiate the TRAPATT plasma state. The capacitance C is provided to supply the current required by the diode to the extent that the transmission line is insufficient. The total capacitance which can be discharged during the short interval of high conduction current in the diode is

$$C_T = C + \tau_P/Z_0$$

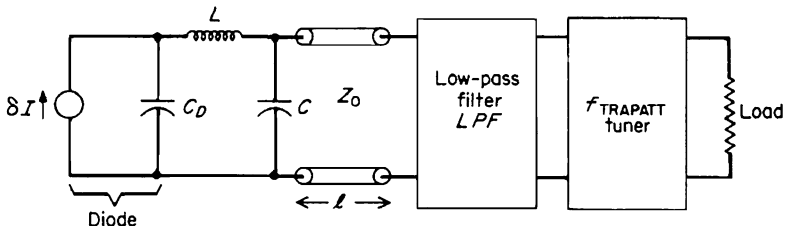

FIGURE 11.6.5 Simplified schematic diagram of TRAPATT circuit.

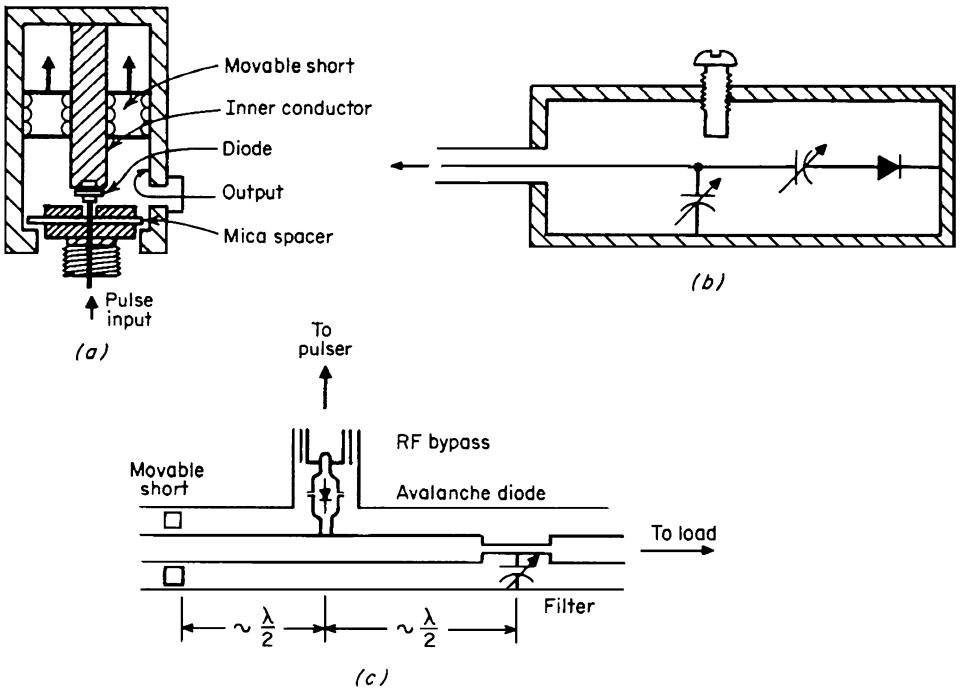

FIGURE 11.6.6 TRAPATT diode circuit arrangements: (*a*) tuned coaxial cavity; (*b*) lumped circuit; (*c*) coaxial circuit.

where τ_P is the time high-current or trapped plasma state exists. τ_P must be at least at large as the transit time of carriers through the diode, thus putting an upper limit on C. This is contrary to the high-current requirements to initially drive the avalanche zone through the diode (10 to 20 kA/cm^2) in large-area devices.

Since the TRAPATT frequency is generally an integral submultiple of the diode transit-time frequency, the line length l ($l = \lambda/2$ at f_{TRAPATT}) presents the low-pass-filter short circuit to the diode as a series resonance at the IMPATT frequency. This net series resonance, however, includes the diode series-reactive elements. Further, this circuit should have a high Q at the transit-time frequency to reduce the buildup time to TRAPATT initiation.

Several TRAPATT circuit configurations are shown in Fig. 11.6.6. The coaxial cavity circuit in Fig. 11.6.6*a* places the diode in the reentrant gap of the half-wave cavity resonator. The output coupling loop passes only the fundamental to a triple stub tuner to match to the load. Proper dc biasing and bypassing are included. This circuit is good into the lower L band. The lumped circuit (Fig. 11.6.6*b*) is compact and very useful for VHF and UHF. The series capacitor is resonated with the inductance of a copper bar and the self-inductance of the diode. The trimmer controls the resonance of the third and fifth harmonics. The circuit of Fig. 11.6.6*c* is a variation on the circuit of Fig. 11.6.4. The use of additional filter sections and/or lumped elements provides better harmonic filtering and results in higher efficiencies. Circuits analogous to those of Fig. 11.6.4, can be implemented in waveguide for the higher frequencies. In all these circuits, the presence of the third and fifth harmonics has been found essential for stable and high-efficiency performance. Higher power levels can be achieved by operating multiple diodes in series and/or parallel configurations.

Another useful technique for extending both power and frequency is the antiparallel diode configuration. The circuit consists of two diodes, placed with opposite polarity approximately one-half fundamental wavelength apart in a transmission line. Operation is similar to a free-running multivibrator. Output may be extracted with a transmission line connected to the midpoint of the diodes, followed by the usual low-pass filter. The position of this filter should be adjusted so that the roundtrip delays from midpoint to diodes and the filter are equal. A microstrip circuit realization for antiparallel operation is given in Fig. 11.6.7.

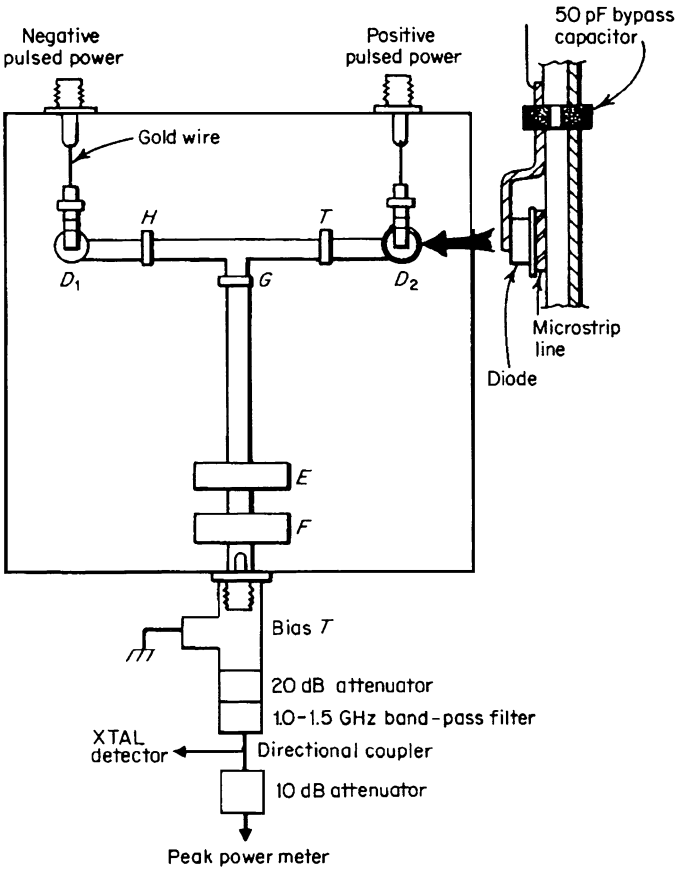

FIGURE 11.6.7 Microstrip version of antiparallel TRAPATT circuit.

Operation of the anomalous avalanche diode for microwave amplification has also been established. A 10-dB dynamic range is typical, with a low-level threshold gain decreasing with increasing power level to a saturated condition. The pulsed bias can be replaced by a simple dc source and storage capacitor. Unlike the *locked-oscillator* mode of operation, only a small residual output is present without the input signal. The locked oscillator will typically display only a 3:1 power change between locked and unlocked cases.

TRAPATT operation has yielded output power levels of 10 to 500 W with efficiencies of 20 to 75 percent in the frequency range from 0.5 to 10 GHz.

BARITT AND DOVETT DIODES

The barrier-injected transit-time (BARITT) diode is the newest active microwave diode. It is similar to the IMPATT diode; however, carriers are injected into the drift zone by a forward-biased junction rather than being extracted from an avalanche region. Holes emitted by the *pn* junction cross the intrinsic region at their saturation velocity and are collected at the *p* contact. The diode behaves as a negative resistance with a phase shift of π rad. BARITT diodes operate at a lower bias voltage and are much lower in noise figure than an IMPATT; however, BARITT diode operating bandwidths are narrow, and output power capability is very low. For C band operation the following results have been attained: 15 dB noise figure and 50 mW output power at 1.8 percent efficiency.

The double velocity transit-time (DOVETT) diode is a new type of BARITT diode. The carrier velocity within a DOVETT diode increases between the injection point and the collection contact. The DOVETT diode has a larger negative resistance than the BARITT diode and therefore operates at higher current density.

TRANSFERRED ELECTRON EFFECT DEVICE (TED) CIRCUITS

This class of circuit, using both the Gunn and limited-space-charge accumulation (LSA) devices depends on the internal negative resistance owing to carrier motion in the semiconductor at high electric fields. When the material is biased above the critical threshold field, a negative dielectric relaxation time is exhibited, which results in amplification of any carrier concentration fluctuations, causing a deviation from space-charge neutrality. The resultant *domain* drifts toward the anode and is extinguished, and a new domain is formed at the cathode. The current through the device consists of a series of narrow spikes with a period equal to the transit time of the domain.

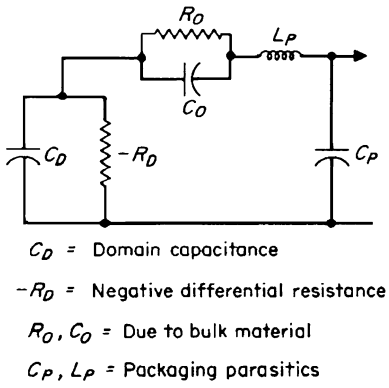

FIGURE 11.6.8 Approximate equivalent circuit of a TED device and its package.

When an rf voltage is superimposed on the bias, in a given period of time, the terminal voltage can be below both the threshold voltage V_{th} and the domain-sustaining voltage V_s. The domain is quenched at any place in the device when the latter occurs, and the nucleation of a new domain is delayed until the voltage again exceeds V_{th}. Therefore the frequency of oscillation is determined by the resonant circuit, including the impedance of the device. Experimental results and computer modeling have shown that the device can be tuned over greater than an octave bandwidth by the external circuit cavity. Although other modes of operation are possible, depending on the characteristics of the external circuit, the LSA mode appears to be the most important.

An approximate equivalent circuit is given in Fig. 11.6.8 with values dependent on frequency, bias, and power level. The capacitance includes the diode static capacitance, in addition to that because of traveling high-field domains.

One of the simplest tuned circuits is the coaxial-line cavity, as shown in Fig. 11.6.9*a*. The diode is mounted concentric with the line, at one end to facilitate heat sinking. The frequency of oscillation is determined

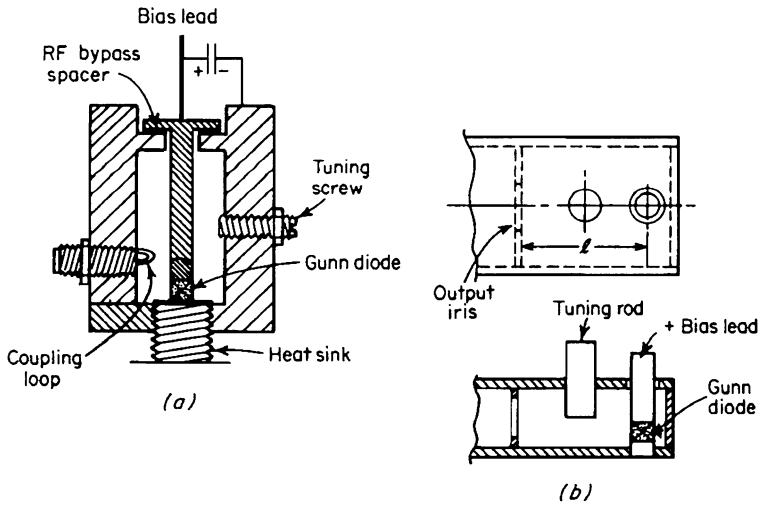

FIGURE 11.6.9 Gunn diode cavity circuits: (*a*) coaxial form; (*b*) waveguide-cavity form.

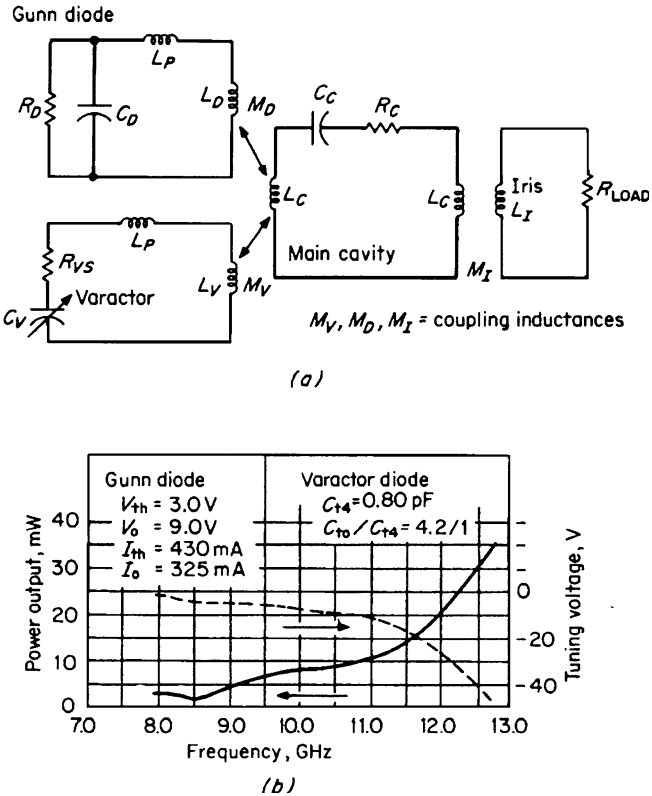

FIGURE 11.6.10 Varactor tuning of Gunn oscillator: (*a*) simplified equivalent circuit; (*b*) tuning characteristic.

primarily by the length of the cavity. The position of the output coupling loop (or plate) determines the load impedance.

A rectangular waveguide cavity configuration (Fig. 11.6.9*b*) is more widely used because of its higher Q and better performance at X band and higher frequencies. The diode post acts as a large inductive susceptance,

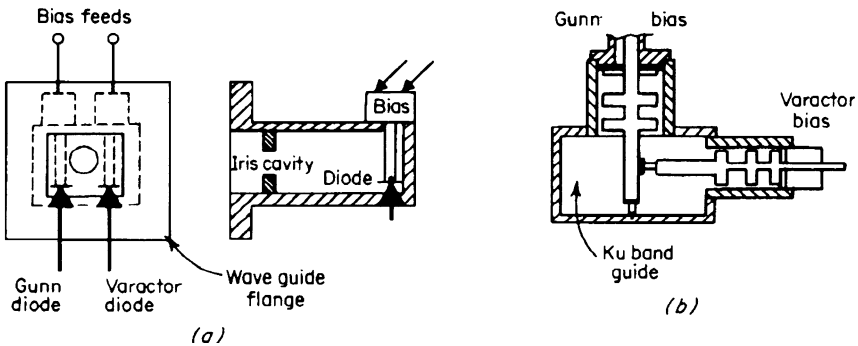

FIGURE 11.6.11 Varactor tuning techniques for Gunn diodes: (*a*) front and side views of double-port waveguide-type; (*b*) type used at K_u band.

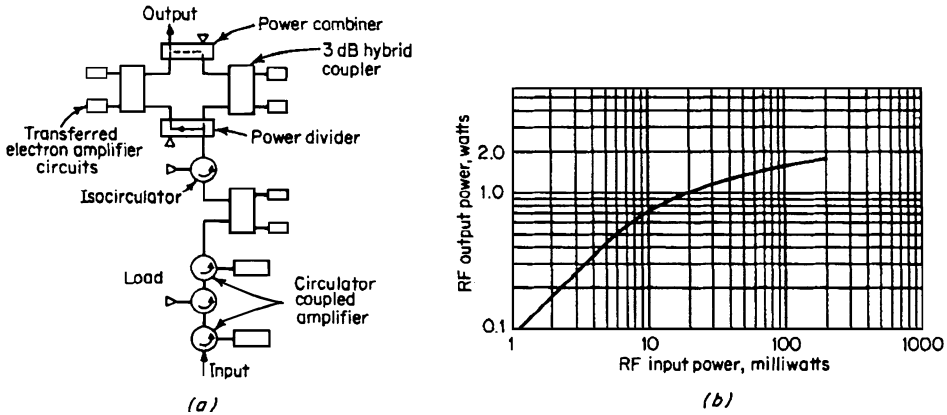

FIGURE 11.6.12 Four-stage ganged TED amplifier chain for 5.7 GHz: (*a*) block diagram; (*b*) power-transfer curve.

which, with the inductive iris, produces the resonant frequency for which the length l is $\lambda/2$. The tuning rod lowers the frequency as its insertion length increases.

In addition to mechanical tuning, both YIG and varactor tuning techniques are applicable. YIG tuning has the potential for the widest tuning range but is limited in tuning speed, hysteresis, and physical bulk. Figure 11.6.10 illustrates a typical varactor-tuned Gunn oscillator equivalent circuit and characteristics. The varactor diode Q is highest at the maximum reverse voltage and decreases with decreasing voltage because of an increase in R_{vs}. Figure 11.6.11 illustrates two varactor-tuned implementation techniques.

The noise characteristic of a GaAs TED is comparable with that of a klystron and is 10 to 20 dB better than an IMPATT diode. Various noise-source models and measuring equipments are discussed in the literature. Several methods can be employed to reduce the AM and FM noise of a Gunn oscillator, including increasing the loaded Q of the cavity circuit: biasing at or near the frequency and/or power turnover points (i.e., bias at which $df/dv = 0$ and $dP_o/dv = 0$); minimizing power-supply ripple; and diode selection.

The TED can also be operated as an amplifier, typically using circulator or hybrid techniques similar to the IMPATT circuits. Parameters of importance are saturation characteristics, bandwidth, gain and phase tracking, linearity, efficiency, and dynamic range. The block diagram of a four-stage chain is shown in Fig. 11.6.12*a*, with operating characteristics in Fig. 11.6.12*b*. Hybrid coupling was found to provide greater linear power output. Gains in excess of 20 dB can be realized. Efficiency and bandwidth are typically less than 10 percent and greater than 35 percent, respectively.

The use of Gunn and LSA diodes extends to frequencies in excess of 90 Hz, with higher peak power capability for the LSA diode than for the IMPATT or for any other Gunn-effect device. TEDs can be operated with a pulsed bias, allowing extremely high power density without damage to the device. Over 1000 W at 10 GHz has been achieved in the LSA mode with short low-duty cycle pulses. Reactive termination and unloading of the circuit at the harmonic frequencies can significantly improve the efficiency. A problem associated with pulsed oscillators is the significant frequency change during each pulse caused by rapid temperature rise. Starting-time jitter can be alleviated by *priming*, i.e., injecting a weak cw signal into the circuit.

TRANSISTOR AMPLIFIER AND OSCILLATOR MICROWAVE CIRCUITS

Silicon bipolar and GaAs FETs are available with cutoff frequencies extending well into X and K_a bands, respectively. Equivalent circuits for these transistor types are given in Fig. 11.6.13. The intrinsic chip element values, with variations considered at low frequencies, are further modified by high-frequency effects.

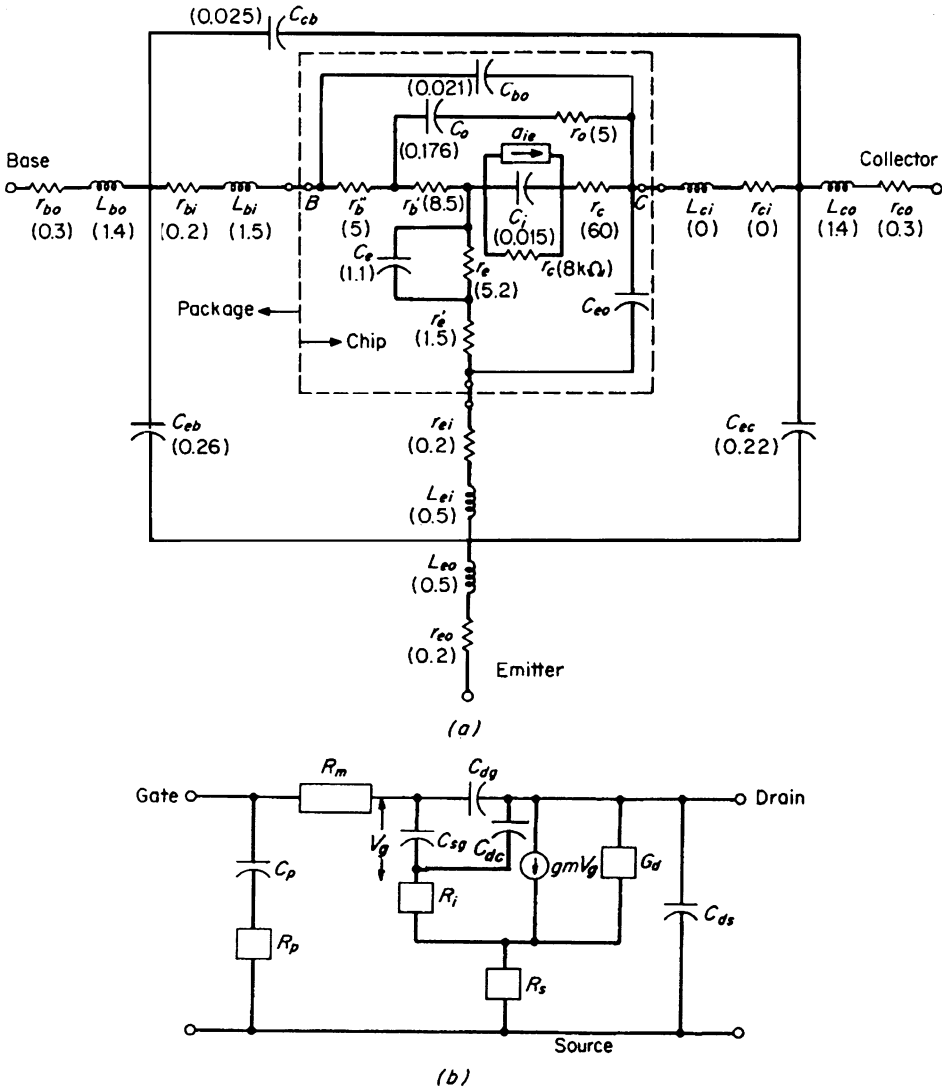

FIGURE 11.6.13 Equivalent circuits of microwave solid-state devices: (*a*) bipolar transistor; (*b*) field-effect transistor (chip only).

A small-signal figure of merit has been defined in terms of the contributing time constants, for a bipolar transistor,

$$K = (\text{power gain})^{1/2}(\text{bandwidth}) = 1/4\pi(r_b'C_c\tau_{ec})^{1/2}$$

where $\tau_{ec} = \tau_e + \tau_b + \tau_l + \tau_c$, τ_e = emitter barrier charging time, τ_b = base transit time, τ_l = collector transit time, and τ_c = collector depletion-layer charging time. The maximum frequency of oscillation is defined as the frequency for which the power gain is unity

$$f_{\max} \approx 1/4\pi(r_b'C_c\tau_{ec})^{1/2}$$

The application of transistors at microwavelengths demands that considerable attention be given to packaging, fixturing, and impedance characterization. Historically, characterization has taken the form of f_T, $r_b'C_c$ specification and/or *h*-*y*-parameter techniques. A more desirable method for high-frequency characterization is by scattering parameters. Scattering parameters describe the relationship between the incident and reflected power waves in any *N*-port network. As such, this technique offers substantial advantages, including remote measurement, broadband (no turning), stability (no short-circuited or open terminations), accuracy, and ease of measurement.

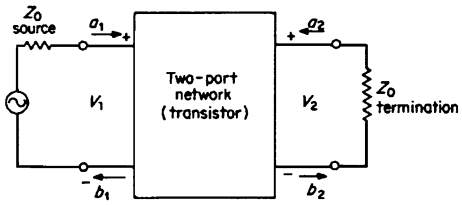

FIGURE 11.6.14 Basic two-port configuration for a microwave transistor.

From Fig. 11.6.14, the scattering equations describing the two-port network can be written.

$$b_1 = S_{11}a_1 + S_{12}a_2 \quad b_2 = S_{21}a_1 + S_{22}a_2$$

Solving for the *S* parameters yields

$$S_{11} = \left.\frac{b_1}{a_1}\right|_{a_2=0} = \text{input reflection coefficient with } Z_L = Z_0$$

$$S_{12} = \left.\frac{b_1}{a_2}\right|_{a_1=0} = \text{reverse transmission gain with } Z_L = Z_0$$

$$S_{21} = \left.\frac{b_2}{a_1}\right|_{a_2=0} = \text{forward transmission gain with } Z_L = Z_0$$

$$S_{22} = \left.\frac{b_2}{a_2}\right|_{a_1=0} = \text{output reflection coefficient with } Z_L = Z_0$$

Other linear two-port parameters can be calculated from *S* parameters (for example, *y* parameters for feedback analysis). Either manual or complex automatic measurement techniques can be used. In either case, the transistor chip package is embedded in a system with a given reference impedance Z_0 and well-defined reference wave planes.

A number of useful relationships can be calculated from the *S* parameters and used in amplifier-oscillator design.

Reflection coefficient-impedance relationship:

$$S_{11} = \frac{Z - Z_0}{Z + Z_0}$$

where Z_0 is the reference impedance.

Input reflection coefficient with arbitrary Z_L:

$$S_{11}' = S_{11} + \frac{S_{12}S_{21}\Gamma_L}{1 - S_{22}\Gamma_L}$$

Output reflection coefficient with arbitrary Z_S:

$$S_{22}' = S_{22} + \frac{S_{12}S_{21}\Gamma_S}{1 - S_{11}\Gamma_S}$$

Stability factor:

$$K = \frac{1 + |D|^2 - |S_{11}|^2 - |S_{22}|^2}{2(S_{12}S_{21})}$$

Transducer power gain:

$$G_T = \frac{|S_{21}|2(1-|\Gamma_S|^2)(1-|\Gamma_L|^2)}{|(1-S_{11}\Gamma_S)(1-S_{22}\Gamma_L) - S_{12}S_{21}\Gamma_L\Gamma_S|^2}$$

Maximum available power gain:

$$G_{\max} = \left|\frac{S_{21}}{S_{12}}(k \pm \sqrt{k^2-1})\right| \qquad \text{for } k > 1$$

Source and load reflection coefficients for simultaneous match:

$$\Gamma_{ms} = M^* \left[\frac{B_1 \pm \sqrt{B_1^2 - 4|M|^2}}{2|M|^2}\right] \qquad \Gamma_{mL} = N^* \left[\frac{B_2 \pm \sqrt{B_2^2 - 4|N|^2}}{2|N|^2}\right]$$

where Γ_S, Γ_L = source and load reflection coefficients

$M = S_{11} - DS_{22}^*$
$N = S_{22} - DS_{11}^*$
$D = S_{11}S_{22} - S_{12}S_{21}$
$B_1 = 1 + |S_{11}|^2 - |S_{22}|^2 - |D|^2$
$B_2 = 1 + |S_{22}|^2 - |S_{11}|^2 - |D|^2$

The maximum power gain is obtained only if the transistor is terminated with the Γ_{ms} and Γ_{mL} resultant impedances. A lossless transforming network is placed between the source and load to realize this transformation.

Generally, the embedding circuits used take the form of simple ladder networks: series-shunt combinations of *L*'s and *C*'s or their transmission-line equivalents. These elements can be determined by moving on the Smith chart from the value of the terminating impedance to the center of the chart along constant resistance-conductance, reactance-susceptance contours for series-shunt elements, respectively. The circuits are typically implemented in strip-line or lumped form, as shown in Fig. 11.6.15.

Optimum design at more than one frequency requires plotting of gain circles at each frequency, with subsequent terminating impedance iteration to obtain the best compromise across the band. Several computer-aided optimization programs are available to simplify this routine. A plot of gain circles and impedance loci for a typical S-band design is shown in Fig. 11.6.16, which corresponds to the collector circuit of Fig. 11.6.15*a*.

NOISE PERFORMANCE OF MICROWAVE BIPOLAR TRANSISTOR CIRCUITS

The noise performance of a well-designed amplifier depends almost entirely on the noise figure of the first transistor. The noise factor of a bipolar transistor amplifier is related to its equivalent circuit parameters and external circuit by

$$NF = 1 + \frac{r'_{bb}}{R_g} + \frac{r_e}{2R_g} + \frac{(r'_{bb} + r_e + R_g)^2}{2r_e R_g h_{feo}}\left[1 + \left(\frac{f}{f_\alpha}\right)^2 (1 + h_{feo})\right]$$

As a result, r'_{bb} should be as low as possible, and the alpha cutoff frequency should be high. The source resistance providing minimum noise figure is

$$R_g\big|_{F\min} = (r'_{bb} + r_e)^2 + \frac{(r'_{bb} + 0.5r_e)(2h_{feo}r_e)}{1+(f/f_\alpha)^2(1+h_{feo})}$$

This value is typically close to the value providing maximum power gain for the common-emitter configuration. Care must be taken in the matching-circuit implementation to minimize any losses in the signal path, e.g., by using high-Q elements and isolated bias resistances. Bipolar junction transistors are available with less than 1 dB noise figure for frequencies below 1 GHz. At 4 GHz the best bipolar transistor noise figure is approximately 3 dB.

HIGH-POWER MICROWAVE TRANSISTOR AMPLIFIERS (USING BIPOLAR TRANSISTORS)

The difficulties arising in power-amplifier operation are because of the nonlinear variation of device parameters as a function of time and to bias conditions. Saturation, junction capacitance-voltage dependence, h_{fe} current (and voltage) level dependence, and charge-storage effects are the prime contributors to this situation. Class A operation is normally not used, implying collector-current conduction angles less than 360°, resulting in further complication of the time-averaging effects. With these qualifications, the basic equivalent circuit given in Fig. 11.6.13*a* applies. Figure 11.6.17*a* shows a greatly simplified equivalent circuit useful for first-order design. Of particular note is the low input resistance, high output capacitance, and a nonnegligible feedback element causing bandwidth, gain, and stability limitations.

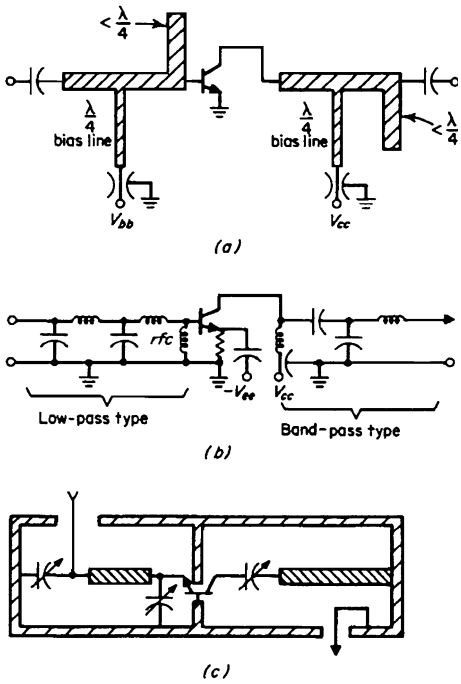

FIGURE 11.6.15 Circuit realizations for microwave transistor circuits: (*a*) strip-line; (*b*) lumped design; (*c*) coaxial design.

Several methods have been used to determine large-signal-device characteristics with varying degree of success. One method involves the measurement of the embedding circuitry at the plane of the transistor terminals, with the transistor removed and the source and load properly terminated. The circuit is tuned for maximum power gain before the transistor is removed to make the measurement. An average or effective device impedance is then the complex conjugate of the measured circuit impedance at that frequency. The maximum power obtainable from a particular transistor is determined by thermal considerations (cw operation), avalanche-breakdown voltages, current-gain falloff at high current levels, and second-breakdown effects.

Bandwidth. The input impedance has been found to be the primary bandwidth-limiting element. R_S varies inversely with the area of the transistor. Hence, for a given package L_S, the Q increases and bandwidth decreases with higher-power transistors

$$Q = \omega_0 L_S/R_S \qquad \text{BW}|_{3\text{ dB}} \approx f_0/Q$$

Impedance matching. The problem of matching complex impedances over a wide band of frequencies has been treated by a number of authors. Essentially, high-order networks can be used to achieve nearly rectangular

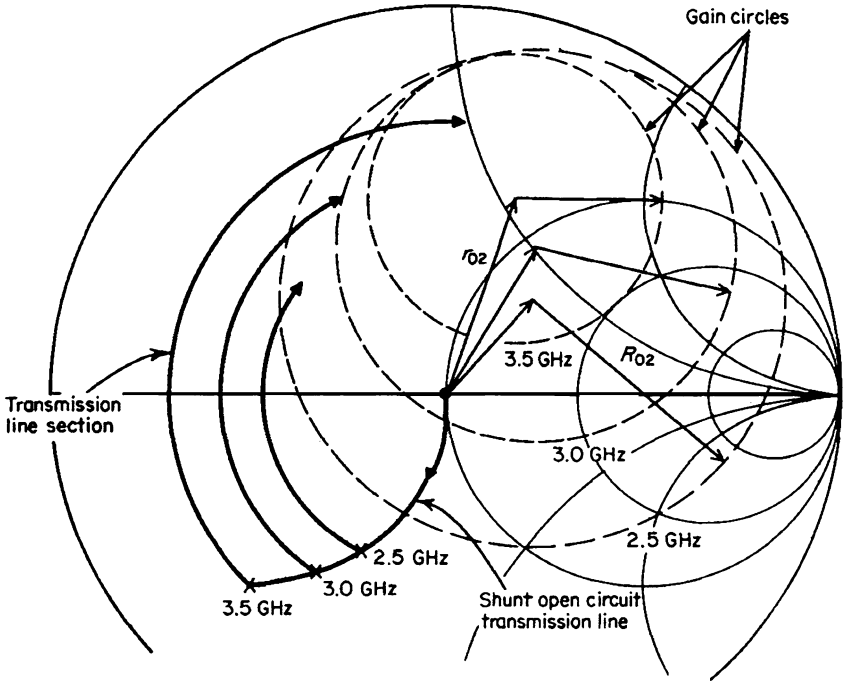

FIGURE 11.6.16 Use of Smith chart in microwave transistor circuit design.

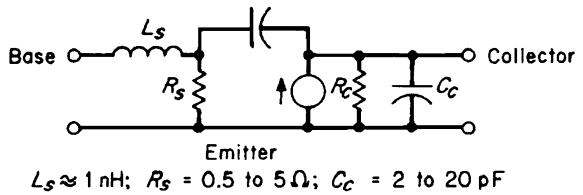

$L_S \approx 1$ nH; $R_S = 0.5$ to 5 Ω; $C_C = 2$ to 20 pF

(*a*)

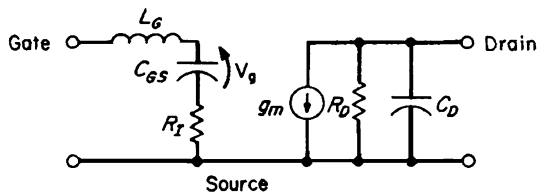

$C_{GS} = 0.2$ to 0.5 pF; $R_I = 10$ to 70 Ω; $R_D = 200$ to 500 Ω

(*b*)

FIGURE 11.6.17 Simplified equivalent circuits of microwave power transistors: (*a*) bipolar transistor; (*b*) FET.

bandpass characteristics. However, without mismatching, the 3-dB bandwidth determined above cannot be extended. In fact, the greater the ratio of generator resistance R_g to transistor input resistance R_S the greater will be the reduction of the intrinsic bandwidth, for a given ripple and number of circuit elements. Hence the external circuit design must consider both the transistor-input-circuit Q value and the impedance level relative to the driving source for a given bandwidth.

Either lumped- or transmission-line-element networks of relative simplicity are typically used to achieve the necessary input-output matching. Although the bandpass type yields somewhat better performance, the low-pass configuration is more convenient to realize physically. Quarter-wave line sections are particularly useful for broadband impedance transformations and bias feed-bypassing functions. Eighth-wave transformers are useful to match the small complex impedances directly without tuning-out mechanisms. The input impedance to a $\lambda/8$ section is real if it is terminated in an impedance with magnitude equal to the Z_0 of the line.

Load resistance. The desired load resistance can be determined to first order by

$$R_L \approx (V_{CC} - V_{CE,\text{sat}})^2/2P_o$$

where P_o is the desired fundamental power output and V_{CC} is the collector supply voltage. This expression is altered by several factors, including circuit Q, harmonic frequencies, leakage, current conduction angle, and so forth. Assuming only the presence of the fundamental frequency, V_{CC} is limited to $^1/_2BV_{CBO}$ by resonant effects. Recently, it has been shown that BV_{CBO} can be exceeded for short pulses without causing avalanche.

Power gain. The power gain depends on the dynamic f_T or large-signal current gain-bandwidth capability, the dynamic input impedance, and the collector load impedance. A simple expression for power gain is

$$\text{PG} = \frac{(f_T/f)^2 R_L}{4R_e(Z_{\text{in}})}$$

The current gain at f_T is of particular importance. The effect of parasitic common-terminal inductance is to reduce this gain in the common-emitter and to cause regeneration in the common-base connection. The latter configuration is more commonly used at frequencies near or above the f_T value, whereas the former generally results in a more stable circuit below f_T. This situation is highly dependent on the parasitic-element situation with respect to the specific frequency. Various forms of instabilities, such as hysteresis (jump modes), parametric, low-frequency, and thermal, can occur because of the parameter values changing with time-varying high-signal levels. Usually, most of these difficulties can be eliminated or minimized by careful design of bias circuits (including fewer elements), ground returns, parasitics, and out-of-band terminating impedances.

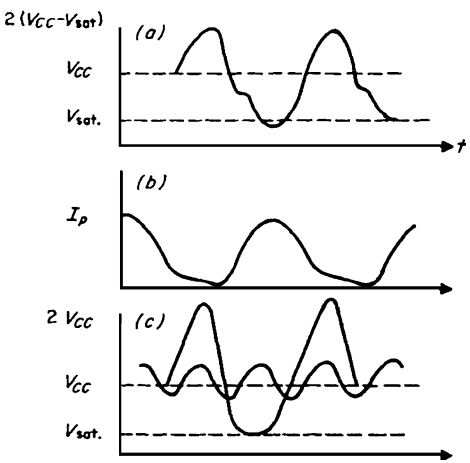

FIGURE 11.6.18 Typical voltage-current waveforms in power applications: (*a*) collector voltage; (*b*) collector current; (*c*) second-harmonic enhancement.

The *collector efficiency* of a transistor amplifier is the ratio of rf power output to dc power input. High efficiency implies low circuit losses, high ratio of output resistance to load resistance, high f_T, and low collector saturation voltage. In addition, experiments and calculations show that for high efficiency, the impedance presented to the collector by the output network should be inductive for the favored generation of second harmonic. If the phase is correct, the amplitude of the fundamental is raised beyond the limit otherwise set by the difference between the supply voltage and $V_{C,\text{sat}}$. Figure 11.6.18 illustrates this effect.

A high value of f_T relative to the operating frequency improves efficiency by causing the operating point to spend less time (per cycle) in the high-dissipation active region between cutoff and saturation. The integrity of the transistor die bond has been found to have a substantial effect on efficiency because of the effects of low intrinsic bulk collector resistance and thermal gradient.

GaAs FIELD-EFFECT TRANSISTOR CIRCUITS

The state of the art of GaAs field-effect transistors for both small-signal and power applications is rapidly improving, thanks to the intrinsically higher carrier mobility in GaAs, coupled with significantly improved fabrication techniques, e.g., in the area of photolithography. Many devices fabricated today use feature sizes as small as 0.25 μm. GaAs FETs are particularly attractive since the parameter values are less variable as a function of operating conditions and their impedances are generally higher than in comparable bipolar devices. As a result, GaAs FET circuits are easier to design and typically achieve lower noise, wider bandwidth, and higher linearity. The common-source configuration has been found to work well for both amplifiers and oscillators.

NOISE PERFORMANCE OF MICROWAVE FET CIRCUITS

The noise figure of an FET can be represented as a minimum noise figure plus a noise factor which depends on the signal source impedance presented to the FET. For an optimum signal source impedance of $R_{SS} + jX_{SS} = R_{OP} + jX_{OP}$, the noise figure is minimized.

$$\mathrm{NF} = F_{\min} + \frac{K_2}{g_m^2}\frac{(R_{SS} - R_{OP})^2 + (X_{SS} - X_{OP})^2}{R_{SS}(R_{OP}^2 + X_{OP}^2)}$$

$$F_{\min} = 1 + K_f(f/f_T)\sqrt{g_m(R_G + R_S)} \qquad K_2 \approx 0.03 \qquad K_f \approx 2.5$$

K_2 and K_f are fitting factors, with K_2 depending on the channel carrier concentrations and dimensions, and K_f depending on the quality of the channel material. The optimum source impedance is

$$R_{SS} = R_{OP} \approx 2.2[1/4g_m + R_G + R_S] \qquad X_{SS} = X_{OP} \approx 160/fC_{GS}$$

It is evident that a low-noise figure requires a high cutoff frequency f_T, and the cutoff frequency is inversely proportional to the gate length. Therefore, a short gate length is important to low-noise operation. The noise figure can also be improved by minimizing the parasitic resistances R_G and R_S.

GaAs FETs are commercially available with noise figures less than 0.5 dB at 4 GHz, less than 1 dB at 8 GHz, and less than 2 dB at 16 GHz.

HIGH ELECTRON MOBILITY TRANSISTORS

The performance of low-noise GaAs FETs is approaching a lower limit because of the finest gate geometry currently attainable (0.25 μm). The new high electron mobility transistor (HEMT) on GaAs offers superior performance because of its carrier transport mechanism, which resembles transport within undoped GaAs, which has little impurity scattering. The structure of an HEMT is similar to a GaAs MESFET, using a heterojunction between GaAs and AlGaAs. The carrier velocity and mobility are twice that of carriers in a MESFET, which results in a higher cutoff frequency and lower noise figure for the same gate geometry. The following results have been achieved with HEMTs: 2 dB noise figure up to 20 GHz without cooling, and 5 dB gain with 7.8 dB noise figure at 71 GHz.

HIGH-POWER MICROWAVE FET AMPLIFIERS

High-power field-effect transistors, like bipolar transistors, exhibit nonlinear device parameter variation with bias conditions. Figure 11.6.17*b* shows a greatly simplified equivalent circuit of a power FET. The parameters C_{GS}, R_I, g_m, R_D, and C_D are bias voltage dependent. The dominant nonlinear effects on power FET operation

are the variation of the channel capacitance C_{GS} with gate and drain bias voltages, the variation of the transconductance g_m with gate voltage, and the variation in drain resistance R_D with drain voltage.

The high-power performance of an FET depends mainly on the gate width, the common lead inductance and other parasitics, the transistor thermal impedance, and the maximum drain voltage capability of the device. The total gate width can be increased by combining a number of individual cells in parallel on one chip. Cells are connected by wire bonding, "flip-chip" mounting techniques, or via-hole connections. A single FET cell may consist of many gate fingers connected in parallel by crossover structures, or wrap-around-plating. Using these techniques total gate widths of 30 mm or more have been attained.

The bias point of the FET has an important effect on the output power capability of the amplifier circuit. The optimum load resistance is determined from the device *I-V* characteristic. V_{GD} is the gate-drain avalanche breakdown voltage when the FET gate is biased at pinch-off (V_P). The limiting drain-source voltage is $V_T = V_{GD} - V_P$. Beyond this voltage, excess current will flow which is unaffected by the input signal at the gate. Therefore, V_L is the level of V_{DS} which corresponds to the maximum rf output power. If V_K is the "knee" drain voltage above which the drain current is approximately flat (independent of drain voltage), then the maximum drain voltage swing can be expressed as $V_L - V_K$ or $V_{GD} - V_P - V_K$. If I_F is the maximum drain current available with a forward-biased gate, then the optimum load resistance for maximum output power is $(V_{GD} - V_P - V_K)/I_F$ and the maximum rf power available to the load is $I_F(V_{GD} - V_P - V_K)/8$.

With a single high-power FET the following cw output power levels can be achieved at 1 dB gain compression: 12 W at 2 GHz, 8 W at 12 GHz, and 1 W at 24 GHz. Efficiencies are typically 25 to 35 percent for class A cw operation. GaAs FETs are commonly used in moderate power applications at microwave frequencies up to 26 GHz. Devices are frequently combined in balanced amplifier circuits to achieve higher output powers. Internally matched chip carrier structures are often used to reduce the effects of package parasitics, and to provide low-loss matching close to the chip. One type of input circuit for an internally matched FET comprises a small SiO_2 chip capacitor connected to the FET gate with a bond wire, forming a π-matching section with the FET input capacitance. Input and output circuits and typically *LC* ladder networks implemented in both discrete and semidistributed circuit forms.

MONOLITHIC MICROWAVE INTEGRATED CIRCUITS

Monolithic circuits, or MMICs, consist of active devices and associated circuitry fabricated together on the same substrate. GaAs MMICs are used to achieve very broad bandwidths and high-frequency operation. Because of the high area of GaAs required and low production yields, MMICs are very expensive. They are best suited to low- and medium-power applications above 20 GHz, where high production volume is expected. The advantages of monolithic circuitry are multioctave bandwidths, millimeter-frequency operation, small size and weight. With MMICs on GaAs the following results have been attained: 4 dB gain, 9 dB noise figure, and +12 dBm output power from 2 to 40 GHz with a distributed amplifier.

TRANSISTOR OSCILLATORS

Transistor oscillators can be designed by choosing the source (or load) terminating impedances such that $S'_{11}\,\Gamma_S \geq 1$ ($S'_{22}\,\Gamma_L \geq 1$). The design is facilitated by plotting stability circles on the Smith chart.

A number of circuit configurations are appropriate, including the standard Colpitts, Hartley, Clapp, coupled-hybrid, and so forth. The major difference, however, is the proper inclusion of device parasitic reactances into the intended configuration. The frequency-determining element(s) may be in the input, output, or feedback circuit but should have a high *Q* for good frequency stability. Care must be taken to decouple or resistively load the circuit at frequencies outside the band where oscillatory conditions are satisfied. This is particularly true for lower frequencies where the current gain is much better.

For bipolar transistors, the common-base and common-collector connections are generally more unstable than common-emitter and most commonly used, depending on the power requirements and frequency of oscillation.

For a GaAs FET oscillator, the device may be in common-source, gate, or drain configuration. The common grounded source arrangement provides the lowest thermal resistance which makes this configuration the

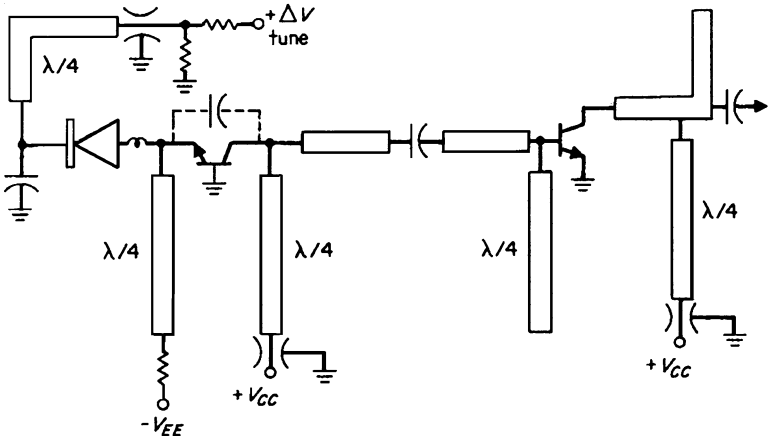

FIGURE 11.6.19 Varactor-tuned microstrip oscillator-buffer circuit.

most likely choice for a power FET oscillator. In the grounded source case a parallel feedback element is used to couple the gate and drain terminals and must be small enough to minimize parasitics.

Transistor oscillators have the advantage of the third terminal which may be used for compensation, modulation, or stabilization. A high-Q cavity resonator is often used in the feedback path for stabilization. The resonator may also be placed between the transistor and the load where it acts as a bandpass filter, or the resonator may be used as a band-reject filter coupled to one oscillator port with the load coupled to the other oscillator port. A high dielectric constant ceramic is usually used for the cavity material to result in a resonator of very small physical size. Barium nanotitanate, which provides a relative dielectric constant of 39, and a Q of up to 8000, is often used as a resonator. Oscillators that use this type of stabilization are called dielectric resonator oscillators, or DROs.

The frequency of an oscillator which is stabilized by a dielectric resonator can be mechanically tuned by varying the gap between the resonator and a metal tuning plate.

Several methods are available to vary the frequency of an oscillator dynamically. Bias variation is effective only over a narrow band and results in substantial power variation. The YIG sphere provides very high Q but is somewhat bulky and of limited tuning speed. The varactor diode provides very low power, octave-tuning bandwidth, and fast tuning in a form compatible with hybrid integration. Figure 11.6.19 shows the schematic of an S-band varactor-tuned wide-band oscillator implemented in hybrid thin-film form. The frequency-determining elements are connected in the high-Q common-base input circuit. This also allows maximum isolation from load mismatch effects (pushing) and permits the balance of the circuitry to be low-Q (broadband).

Both high- and low-power oscillators are large-signal; i.e., the output power is limited primarily by beta falloff, with increasing current at a given frequency and collector voltage.

Bipolar transistors are generally used for oscillators up to X band. Output powers of +16 dBm at 8 GHz and +7 dBm at 13 GHz have been achieved with bipolar transistor oscillators by using a finline mount. The near carrier noise for the silicon bipolar transistor was 10 to 20 dB better than the noise characteristic of an FET oscillator operating at the same frequency.

The maximum frequency of oscillation of a GaAs FET is about 80 GHz for a 0.25 μm gate length. The following results have been attained at 35 GHz: +1 dBm output power and noise-to-carrier ratios of –78 dBc/Hz at 10 kHz and –87 dBc/Hz at 25 kHz.

TRAVELING-WAVE-TUBE CIRCUITS

The traveling-wave tube is a unique structure capable of providing high amplification of rf signals varying in frequency over several octaves without the need for any tuning or voltage adjustment (Sec. 7). Figure 11.6.20

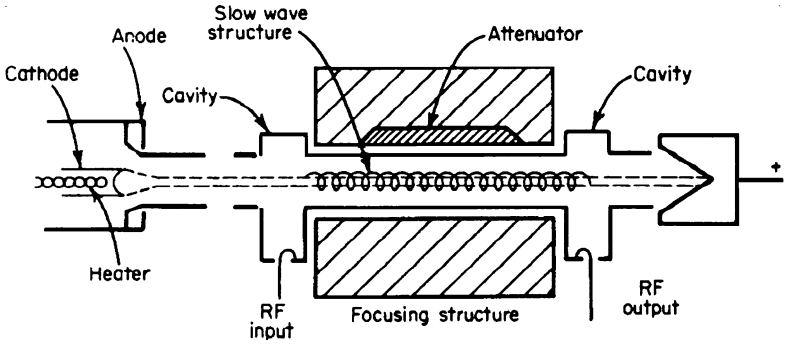

FIGURE 11.6.20 Traveling-wave amplifier circuit.

shows the principal components of an amplifier using this tube. Electrons emitted by the electron-gun assembly are sharply focused, drawn through the length of the slow-wave rf structure, and eventually dissipated in the collector. Synchronism between the rf electromagnetic wave and the beam electrons results in a cumulative interaction which transfers energy from the dc beam to the rf wave. For details on this type of amplifier see Sec. 7.

Figure 11.6.21 shows the gain characteristics of a typical broadband TWT amplifier. As more energy is extracted from the electron beam, it slows down. This loss of synchronism results in lower gains at higher power levels. One advantage of this overdrive characteristic is the protection of following stages against strong signals.

Traveling-wave tube amplifiers provide high gain for signals up to about 30 GHz. Power TWT technology is still advancing. TWTs are available with as high as 30 W cw output power at 12 GHz and 42 percent efficiency. Long-term reliability and noise figure remain poor in comparison to most solid-state devices.

The *backward-wave oscillator* is essentially a TWT device making use of the interaction of the electron stream with an electromagnetic wave whose phase and group velocities are 180° apart. At a sufficient beam current, oscillations are produced as discussed above, without a reverse-wave attenuator. These devices are

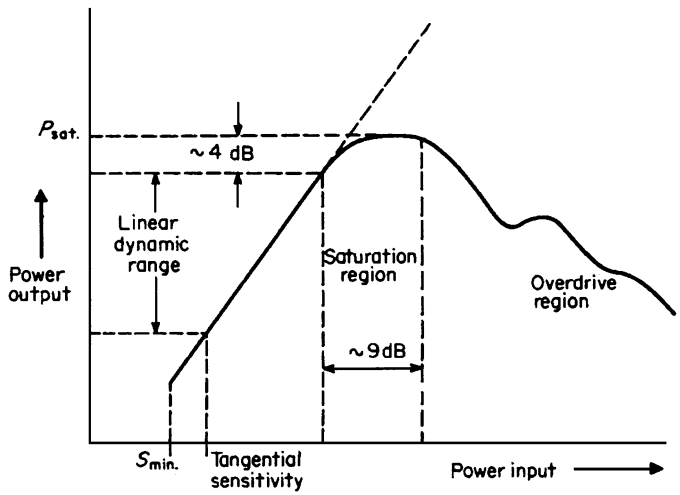

FIGURE 11.6.21 Typical gain characteristic of a broadband TWT amplifier.

voltage-tunable. Frequency is proportional to the half power of the cathode-helix voltage and the dimensions of the structure. Multioctave tuning is possible, depending on output-power-variation requirements. These oscillators have low pulling figures and, typically, high pushing figures. Frequency stability is excellent, usually dependent on power-supply variations. These devices are typically low power (<1 W).

KLYSTRON OSCILLATORS AND AMPLIFIERS

The chief advantages of the klystron amplifier oscillator are that it is capable of large stable output power (10 MW) with good efficiency (40 percent) and high gain (70 dB). Basically, the mechanism involves modulation of the velocity of electrons in a beam by an input rf signal. This is converted into a density-modulated (bunching) beam from which a resonant cavity extracts the rf energy and transforms it to a useful load.

Klystron amplifiers can be conveniently divided into three categories: (1) two-resonator single-stage high- and low-noise voltage amplifiers, (2) two-resonator single stage (*optimum bunching*) power amplifiers, and (3) multiresonator cascade-stage voltage and power amplifiers. The power gain of a two-cavity voltage amplifier can be given by

$$G = \frac{M_1^2 N_2^2}{240\beta}\left(\frac{\pi a}{\lambda}\right)^2 \frac{G_0}{(G_{BR})^2}$$

where M_1, M_2 = beam coupling factors
a = beam radius
G_0 = beam conductance
G_{BR} = cavity shunt conductance contributions because of beam loading and ohmic losses
β = (electron velocity)/(velocity of light)

A simplified schematic representation of a klystron amplifier is shown in Fig. 11.6.22. Multicavity tubes are typically used for high pulse power and cw applications. The intermediate cavities serve to remodulate the beam, causing additional bunching and higher gain-power output. Optimum power output is obtained with the second cavity slightly detuned. Further, loading of this cavity serves to increase the bandwidth (at the expense of gain). These tubes typically use magnetically focused high-perveance beams.

The broadbanding of a multicavity klystron is accomplished in a manner analogous to that of multistage i.f. amplifiers. A common technique is stagger tuning, which is modified somewhat, because of nonadjacent cavity interactions.

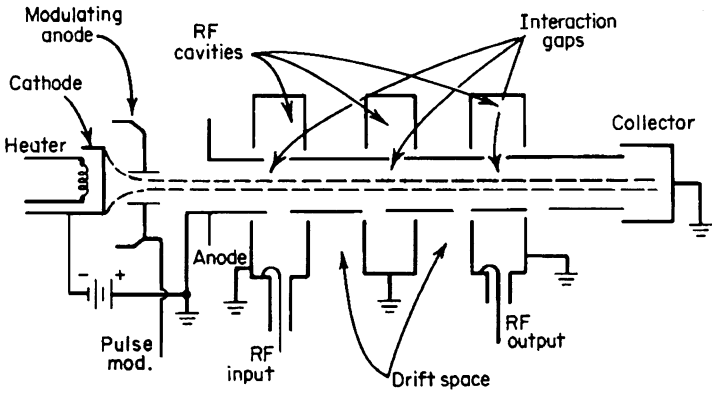

FIGURE 11.6.22 Klystron amplifier structure.

The two-cavity amplifier can be made to oscillate by providing a feedback loop from output to input with proper phase relationship. Klystrons can also be used for frequency multiplication, using the high harmonic content of the bunched-beam current waveforms.

Reflex Klystron

A simple klystron oscillator results if the electron-beam direction is reversed by a negative electrode, termed the *reflector*. A schematic diagram of such a structure is given in Fig. 11.6.23. Performance data for a reflex klystron are usually given in the form of a reflector-characteristic chart. This chart displays power output and frequency deviation as a function of reflector voltage. Two distinct classes of reflex klystrons are low-power tubes for oscillator, pump, and test applications and higher-power tubes (10 W) for frequency-modulator applications. Operating voltage varies from 300 to 2000 V with bandwidths up to ~200 MHz.

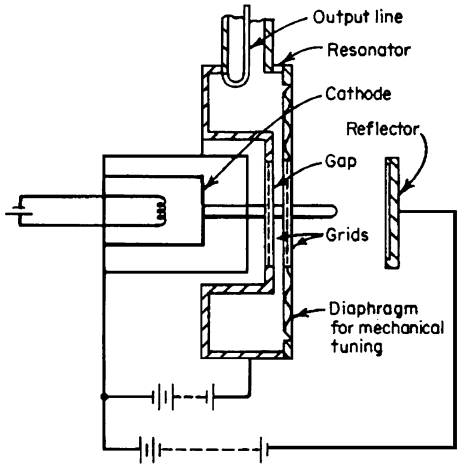

FIGURE 11.6.23 Reflex klystron with coaxial-line loop output.

CROSSED-FIELD-TUBE CIRCUITS

Practically all crossed-field tubes have integrally attached distributed constant circuits. Operation within a critical range of beam current is necessary to maintain the proper bandpass characteristics.

Magnetron

The original microwave tube was a magnetron diode switch with oscillations owing to the cyclotron resonance frequency. Several oscillator circuits were used until the standard cavity-resonator magnetron was introduced in 1940.

The relations between power, frequency, and voltage versus the load admittance are shown in the Rieke diagram (Fig. 11.6.24). Such charts illustrate the compromises necessary to obtain desired operating conditions. In general, good efficiency results from increasing anode current and magnetic field strength.

Various load effects can be considered with the Rieke diagram. The pulling figure [measure of frequency change for a defined load mismatch – (SWR) = 1.5 at all phase angles] and long-line effect are examples.

The area of highest power on the Rieke diagram is called the *sink* and represents the tightest load coupling to the tube. The highest efficiency results in this region; however, a poor spectrum or instability typically results. The buildup of oscillations in the antisink region is closer to ideal; however, this lightly loaded condition may also result in instability. Stability is a measure of the percentage of missing pulses, usually defined at 30 percent energy loss.

Tuning

Methods used to tune a magnetron are classified as mechanical, electronic, and voltage tuning. In the mechanical methods, the frequency of oscillation is changed by the motion of an element in the resonant circuit. Two types are shown in Fig. 11.6.25. An electron beam injected into the cavities will change the effective dielectric constant and hence the frequency. By using the frequency pushing effect it has been possible to tune the magnetron over a frequency range of 4 to 1 (typically, 0.1 to 2 MHz/V) using voltage tuning. The frequency change is usually linear, but the power output is not constant over the tuning range. Magnetrons with power output greater than 5 MW and efficiencies 50 percent or more are available.

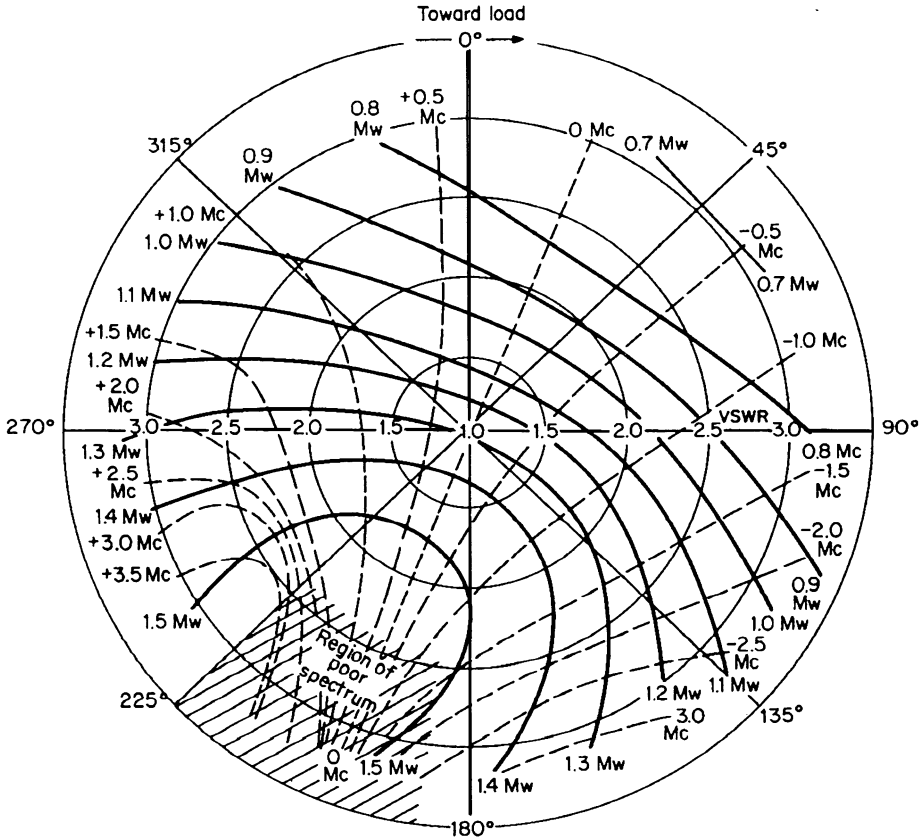

FIGURE 11.6.24 Rieke diagram for an L-band magnetron at 1250 MHz. Solid curves are contours of constant power; dashed curves of constant frequency. (*Raytheon Company*.)

Amplitron

The Amplitron is essentially a magnetron with two external couplings, enabling amplifier operation. It is characterized by high power, broad bandwidth, very high efficiency, and low gain. The output is independent of rf input but dependent on dc input. It acts as a low-loss passive transmission line in the absence of high voltage. A typical plot of power for an Amplitron is shown in Fig. 11.6.26. Conversion efficiency of an Amplitron can be as high as 85 percent. The gain can be increased by inserting mismatches into the input and output transmission lines.

GYROTRON CIRCUITS

Beyond 30 GHz, the power available from classical microwave tubes declines sharply. The gyrotron offers the possibility of high power at millimeter wave frequencies.

The gyrotron is a cyclotron resonance maser. The structure of the gyrotron includes a cathode, a collector, and a circular waveguide of a gradually varying diameter. Electrons are emitted at the cathode with small variations in speed. The electron current density is very high. The electrons are accelerated by an electric field and guided by a static magnetic field. The nonuniform induction field causes the rotational

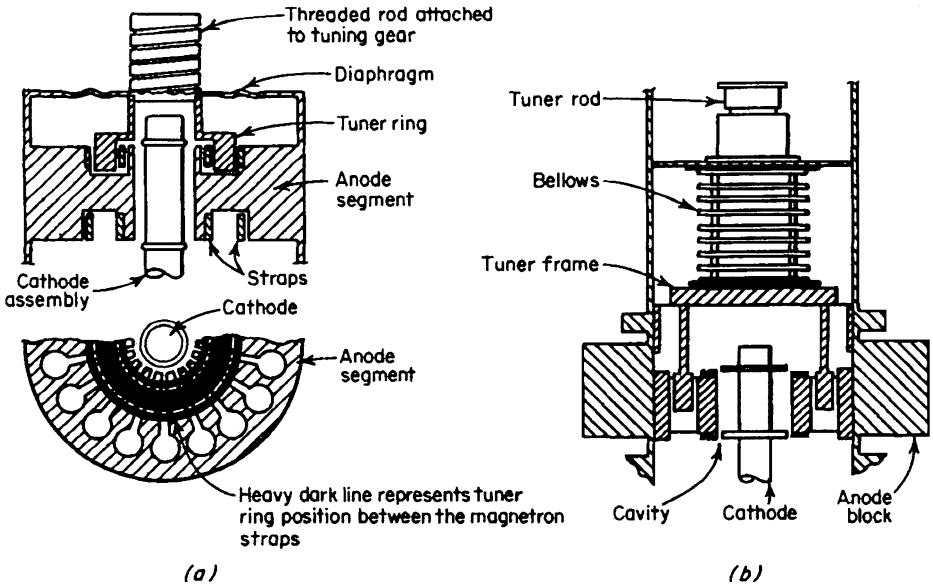

FIGURE 11.6.25 Mechanical magnetron tuning mechanisms: (*a*) capacitance type; (*b*) inductance type.

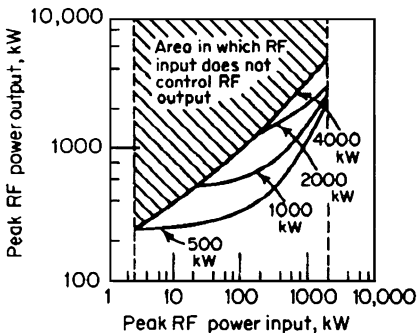

FIGURE 11.6.26 Gain characteristic of model QK520 L-band amplifier.

speed of the electrons to increase, which in turn causes the linear velocity of the electrons to decrease, while they follow a helical trajectory. The microwave field exists within the circular waveguide, where the cutoff of the mode is only slightly above the microwave signal frequency. The electrons give up energy because of interaction with the field of the rotating mode. This causes bunching of the electrons, similar to the bunching within a klystron. Finally there is a decompression zone where the induction decreases and the electrons are collected.

The smooth shape of the gyrotron circular waveguide produces less loss than other microwave tubes. The power available with a gyrotron is 100 or more times greater than that available from classical microwave tubes at the same frequency. The output power levels which can be attained with a gyrotron in cw operation are as follows: 12 kW at 107 GHz and 31 percent efficiency, or 1.5 kW at 330 GHz and 6 percent efficiency.